

Published in final edited form as:

*Nature*. 2009 January 15; 457(7227): 313–317. doi:10.1038/nature07487.

## Experience leaves a lasting structural trace in cortical circuits

Sonja B. Hofer<sup>1,2</sup>, Thomas D. Mrsic-Flogel<sup>1,2</sup>, Tobias Bonhoeffer<sup>1</sup>, and Mark Hübener<sup>1</sup>

<sup>1</sup> Max Planck Institute of Neurobiology, D-82152 Martinsried, Germany

### Abstract

Sensory experiences exert a powerful influence on the function and future performance of neuronal circuits in the mammalian neocortex<sup>1-3</sup>. Restructuring of synaptic connections is believed to be one mechanism by which cortical circuits store information about the sensory world<sup>4,5</sup>. Excitatory synaptic structures, such as dendritic spines, are dynamic entities<sup>6-8</sup> which remain sensitive to alteration of sensory input throughout life<sup>6,9</sup>. It remains unclear, however, whether structural changes at the level of dendritic spines can outlast the original experience and thereby provide a morphological basis for long-term information storage. Here we follow spine dynamics on apical dendrites of pyramidal neurons in functionally-defined regions of adult mouse visual cortex during plasticity of eye-specific responses induced by repeated closure of one eye (monocular deprivation, MD). The first MD episode doubled the rate of spine formation, thereby increasing spine density. This effect was specific to layer 5 cells located in binocular cortex where most neurons increase their responsiveness to the non-deprived eye<sup>3,10</sup>. Restoring binocular vision returned spine dynamics to baseline levels, but absolute spine density remained elevated and many MD-induced spines persisted during this period of functional recovery. Remarkably, spine addition did not increase again when the same eye was closed for the second time. This absence of structural plasticity stands out against the robust changes of eye specific responses which occur even faster upon repeated deprivation<sup>3</sup>. Thus, spines added during the first MD experience might provide a structural basis for subsequent functional shifts. These results provide a strong link between functional plasticity and specific synaptic rearrangements, revealing a mechanism of how prior experiences could be stored in cortical circuits.

---

Temporary closure of one eye induces adaptive changes of eye-specific responses in binocular visual cortex of juvenile<sup>11-14</sup> and adult mice<sup>3,10,15,16</sup>, as neurons shift their preference towards the non-deprived eye. These ocular dominance (OD) shifts can be reverted fully by restoring binocular vision, and they become accelerated when the animal experiences a second MD episode several weeks after the first<sup>3</sup>. Thus, a transient adaptation to altered visual input leaves a ‘trace’ in cortical circuits which facilitates similar adaptations in the future. While this trace could take on multiple forms, here we investigate whether it could be morphological in nature, whereby potential synaptic restructuring during the initial experience<sup>17</sup> outlasts the functional changes to support later OD shifts.

---

Users may view, print, copy, and download text and data-mine the content in such documents, for the purposes of academic research, subject always to the full Conditions of use:[http://www.nature.com/authors/editorial\\_policies/license.html#terms](http://www.nature.com/authors/editorial_policies/license.html#terms)

Correspondence should be addressed to M.H. (mark@neuro.mpg.de).

<sup>2</sup>Present address: Department of Physiology, University College London, London, WC1 6JJ, UK

We repeatedly imaged apical dendritic stretches of layer 5 (L5) and layer 2/3 (L2/3) pyramidal neurons in functionally defined regions of mouse visual cortex by combining two-photon laser scanning microscopy with optical imaging of intrinsic signals. Adult mice (P 45-100) expressing eGFP sparsely in the cortex<sup>18</sup> were implanted with a glass window<sup>6</sup> through which the position of binocular visual cortex was first determined functionally by intrinsic signal imaging (Fig. 1a,b). Subsequently – starting on average 16 days after surgery – spine dynamics of labelled neurons in different cortical regions (see Suppl. Fig. 1 for positions of imaged neurons) were followed for up to 8 weeks. Dendrites were imaged in layer 1 at 4-day intervals while animals experienced repeated episodes of MD separated by a period of normal binocular vision (Fig. 1, Suppl. Fig. 2a). We also corroborated our previous findings on facilitated functional plasticity during repeated MD<sup>3</sup> in adult mice implanted with cranial windows: OD shifts caused by the first MD, as measured by intrinsic signal imaging, reversed completely after re-opening the deprived eye. A second MD of 3 days in the same eye induced a stronger OD shift than the first 3-day MD ( $p=0.009$ , Fig. 1c, Suppl. Fig. 2c, Suppl. Fig. 3a,b).

Chronic two-photon imaging revealed that under normal conditions,  $5.6 \pm 0.4\%$  (mean  $\pm$  SEM) of spines appeared (spine gain) and  $6.7 \pm 0.4\%$  of spines disappeared (spine loss) on apical dendrites of L5 pyramidal neurons in the binocular visual cortex over a 4-day period (Fig. 1d,e). Closing the eye contralateral to the imaged hemisphere increased spine addition rate in the binocular region already during the first 4 days of deprivation and, to a lesser degree, during the subsequent 4 days of MD, compared to baseline conditions or control animals (Fig. 1e,h, MD 0-4d:  $p<0.002$ , MD 4-8d:  $p<0.03$ ). Spine elimination rate, however, was not consistently altered by MD, with marginally fewer spines disappearing during the first 4 days of deprivation (Fig. 1e,  $p=0.03$ , compared to baseline conditions, for a comparison of gain and loss in individual neurons see Suppl. Fig. 4a). Consequently, spine number was increased by  $\sim 8\%$  at the end of the 8d MD period (before MD:  $399 \pm 12.6$  spines/mm, 8d MD:  $434 \pm 11.9$  spines/mm,  $p<0.002$ , see also Fig. 3). Notably, L5 neurons with more complex apical dendrites displayed a larger increase in spine density during MD than neurons with simpler apical structures ( $p<0.001$ , see Suppl. notes and Suppl. Fig. 4b).

The selective increase in spine number could reflect either the reorganization of synaptic inputs associated with OD shifts, or a non-specific, compensatory effect due to the loss of visual drive through the deprived-eye. To distinguish between these possibilities, we quantified spine dynamics on neurons located in regions surrounding the binocular cortex. Neurons in monocular primary visual cortex, which receive input exclusively from the deprived eye, did not exhibit changes in spine turnover as a consequence of visual deprivation (Fig. 1f). Similarly, spine dynamics of neurons located laterally or frontally, outside of the functionally defined borders of the binocular cortex, presumably in monocular parts of higher visual areas<sup>19</sup> (see Suppl. Fig. 1), did not change during MD (Suppl. Fig. 5). And finally, neurons positioned at the border regions of the binocular cortex showed an intermediate effect: The rate of spine addition increased only after 8 days of MD (Fig. 1g, MD 4d:  $p>0.2$ , MD 8d:  $p<0.02$ ). Therefore, the observed increase in spine number was specific to binocular cortex, indicating that the experience of imbalanced input from the eyes causes synaptic reorganization accompanying OD shifts in mature visual cortex. Overall, the net addition of spines during MD parallels closely the functional consequences of adult MD,

whereby open-eye responses are selectively strengthened<sup>3,10,20</sup> (Suppl. Fig. 3a,b). Conversely, the negligible loss of spines matches the absence of substantial deprived-eye response weakening during adult OD plasticity<sup>3,10,20</sup>.

We imaged a subset of mice at 2-day intervals during MD to obtain a closer correlation between spine gain and OD shifts (Suppl. Fig. 3c). Most new spines appeared during a time when the strongest functional changes occurred, between day 2 and 4 of MD, while after day 6, when the OD shift had reached saturation<sup>3</sup> (Fig. 1c) spine gain returned to baseline levels. The consistency between structural and functional data suggests that synaptic remodelling, implemented by the addition of new spines on L5 neurons, contributes to the strengthening of non-deprived eye representation in binocular cortex.

In contrast to L5 neurons, spine dynamics on apical dendrites of L2/3 neurons did not change significantly during MD (Spine gain:  $p > 0.4$ , spine loss:  $p > 0.06$ , Fig. 2). As cells in L2/3 exhibit robust OD shifts<sup>3,15,16</sup> in adults, more pronounced structural changes might occur on deeper parts of the dendritic trees<sup>17</sup> or different mechanisms of OD plasticity might prevail in the upper layers of mature visual cortex.

In adult mice, restoring binocular vision leads to complete functional recovery from an OD shift within a week following a 7-day MD<sup>3</sup> (Fig. 1c). To determine whether MD-induced spine changes are also reversed during recovery, we reopened the deprived eye and continued imaging the same dendritic stretches on L5 neurons. The rate of spine formation in binocular cortex returned to baseline levels already within 4 days after reopening the contralateral eye (Fig. 1e), while the rate of spine loss did not change ( $p > 0.3$ , Fig. 1e), resulting in spine numbers which remained elevated even after recovery from MD. To demonstrate that MD-induced structural changes indeed outlast the experience, we analyzed data from only those cells which had been imaged over the entire recovery period following MD and which showed a clear change in spine dynamics during MD (14 cells, 9 mice). The average spine density, which had increased progressively during the 8-day MD episode, declined only modestly in the following period of binocular vision (Fig. 3a,b). Two weeks later, spine densities were still substantially higher than prior to MD or compared to control animals ( $p < 0.005$ , Fig. 3b). Tracking the long-term fate of individual spines revealed that the density of new spines that appeared during the 8 days of MD and remained stable over the entire period of binocular vision following MD (“persistent new spines”<sup>21</sup>) was more than 2-fold higher than that of control mice during a similar time period and than that of spines gained in the 8-day baseline period before MD ( $p < 0.001$ , Fig. 3c). Interestingly, the relative fraction of new spines that persisted during the weeks following MD was not significantly increased ( $p > 0.05$ , Fig. 3d), indicating that the conversion efficiency of new spines into persistent spines was no different between control and deprived mice. In summary, MD in adult mice increases the number of spines, many of which remain when normal vision is restored. Thus, a structural correlate of the altered experience persists, even though changes in eye-specific response strength elicited by MD are completely reversed during recovery<sup>3</sup>.

Inspired by the work of Eric Knudsen’s group on plasticity in the barn owl midbrain<sup>22,23</sup> we had previously shown that closure of the same eye for a second time leads to a faster and more persistent OD shift<sup>3</sup> (Fig. 1c). Could the extra spines induced by one MD episode

represent the lasting ‘memory trace’ of earlier experience? To test this, we induced a second MD of the same eye after a 2–3 week period of normal vision. Remarkably, the second MD did not alter spine dynamics, nor increase spine density on L5 neurons in binocular cortex ( $p > 0.2$ , Fig. 4a,c). This striking difference in structural plasticity compared to the first MD could not be accounted for by older age, longer time since cranial window implantation, or the number of imaging sessions prior to the second deprivation episode: control mice matched for these parameters, which experienced only a single MD, showed altered spine dynamics ( $p < 0.02$ , Fig. 4b) and increased spine density similar to that observed during the first MD in animals undergoing repeated MD ( $p > 0.7$ , Fig. 4d, compare to **Fig. 1e** and **3b**).

The absence of structural plasticity during the second MD strongly contrasts the presence of robust and even enhanced functional plasticity upon repeated MD (Fig. 1c). When induced in adult mice, these OD shifts are implemented primarily by strengthening of non-deprived eye responses<sup>3</sup> (Suppl. Fig. 3b). The new spines formed during the first MD likely carry synapses<sup>24,25</sup>, presumably contributing to the strengthening of non-deprived eye responses. We suggest that these synapses are then weakened or silenced after eye re-opening – without withdrawal of the spines – thereby enabling full recovery of eye-specific responses. Their potentiation or re-activation might later allow for faster strengthening of non-deprived eye responses during the second MD, since physical connections do not have to be re-established.

A robust correlation between spine size and synapse size and strength has been established in the literature<sup>26,27</sup>, and strengthening or weakening of synaptic transmission has been shown to lead to spine enlargement or shrinkage, respectively<sup>28–30</sup>. We therefore followed the size of individual spines that appeared during MD and outlasted this experience by measuring their integrated brightness (see methods). On average, new spines became larger during deprivation and were of similar size as new spines in control animals ( $p = 0.12$ , MD spines:  $50.0 \pm 24.1$ ,  $n = 34$ ; control spines:  $57.3 \pm 18.2$ ,  $n = 19$ ; mean brightness  $\pm$  SEM) and as other spines in the vicinity ( $p = 0.38$ ,  $63.1 \pm 46.0$ ,  $n = 130$ ). However, spines that appeared during MD shrank after binocular vision had been restored and, importantly, their size increased again during the second MD (ANOVA,  $p = 0.0002$ , Fig. 4e,f, Suppl. Fig. 6). In contrast, persistent new spines in control animals grew and stabilized after their appearance (ANOVA,  $p = 0.72$ , Fig. 4f, Suppl. Fig. 6). Thus, size changes of MD-induced spines correlate with the potentiation, depression and re-potentiation of non-deprived eye responses during MD, recovery and second MD, respectively, thereby supporting the idea that these new spines are functionally important as they are likely to bear synapses whose strength is modulated by visual experience. In the future, calcium imaging in individual spines *in vivo* during eye-specific visual stimulation might provide final proof of the nature of synaptic inputs on these spines.

Overall, our experiments not only show that the rearrangement of intracortical connections by way of dendritic spines is one mechanism contributing to experience-dependent plasticity, but also that these spines embody the history of previous adaptations by cortical circuits. In this way, specific structural modifications might serve to store information about past experiences and thereby endow the cortex with an improved ability to adapt to similar experiences in the future.

## Methods summary

Adult mice expressing eGFP in a small subset of cortical neurons (GFP-M line18) were implanted with a chronic imaging window<sup>6</sup> over the right visual cortex. Optical imaging of intrinsic signals during presentation of small, rapidly changing, drifting-grating stimuli was used to identify functionally the binocular region and to assess eye-specific responses and OD after different durations of MD, after re-opening of the eye and after a second MD, as described previously<sup>3</sup>. Apical dendritic stretches, 10 to 100  $\mu\text{m}$  below the cortical surface, of layer 5 and layer 2/3 pyramidal neurons were repeatedly imaged every 4 days or every 2 days under ketamine/xylazine anaesthesia with two-photon laser scanning microscopy (custom-built microscope, Mai Tai Spectra-Physics Ti:sapphire laser at 910 nm, 40 $\times$  IR Olympus objective). Spine dynamics were followed during alternating periods of normal, binocular vision and 8-day periods of contralateral eyelid suture. In total, 10548 spines from 100 cells were tracked over 5-14 imaging sessions. The percentage of spines appearing and disappearing on a cell in between two successive imaging sessions relative to the total spine number of the previous imaging session was defined as the rate of spine gain and spine loss, respectively. For spine size measurements, the integrated brightness of all pixels comprising the spine was calculated (see methods). P-values were calculated with a non-parametric Wilcoxon rank sum test or Dunnett test for independent samples, and with a repeated measures analysis of variance and Wilcoxon sign rank test for paired samples.

## Methods

### Window implant surgery

C57/Bl6 mice (postnatal day (P) 45 – 100) expressing eGFP under the Thy-1 promoter in a small subset of cortical neurons (GFP-M line18) were anaesthetized with an intraperitoneal injection of ketamine (0.14 mg per g bodyweight) and xylazine (0.01 mg per g bodyweight). Atropine (0.01 ml at 0.1 mg/ml) and fortecton (0.01 ml at 2 mg/ml) were injected subsequently. After resecting the scalp and cleaning the skull, a circular craniotomy (3-4 mm diameter) was performed over the posterior part of the right hemisphere. The intact dura was covered with a thin layer of agarose (1.2% in ACSF) and a glass coverslip (No.1, 5 mm diameter). Dental acrylic was applied to seal implant, skull and wound margins. A small metal bar was embedded in the acrylic for fixing the animal during imaging sessions. Animals were housed separately after surgery.

### Intrinsic signal imaging

In all mice the binocular region of the visual cortex was identified using optical imaging of intrinsic signals. In a subset of animals, shifts in OD were determined during repeated episodes of MD (for details see ref. 3). Mice were anaesthetized with a mixture of Fentanyl (0.05 mg/kg), Midazolam (5.0 mg/kg) and Medetomidine (0.5 mg/kg). Rectangular square-wave drifting gratings of changing orientations (0.03 cycles/ $^{\circ}$ , 2 cycles/s, 25 $^{\circ}$  $\times$ 25 $^{\circ}$  for identifying the binocular cortex, 18 $^{\circ}$  $\times$ 18 $^{\circ}$  for OD measurements) were presented to the eyes independently at neighboring positions on a monitor in the central visual field of the mouse. Images (600 ms duration) of the cortex through the cranial window were taken with a cooled, slow-scan CCD camera under 707 nm-light illumination. Three 'blank' images were

acquired before the stimulus was shown for 7 s. Response maps were blank-corrected and averaged over 9-24 stimulus repetitions. Responses were combined in a maximum-response projection to visualize the binocular visual cortex. Response strength for the two eyes was determined as described before<sup>3</sup>. The ratio of contralateral to ipsilateral eye response strength (contra/ipsi ratio) was calculated as a measure for ocular dominance.

### Two-photon imaging and lid suture

Using two-photon laser scanning microscopy, dendritic stretches of layer 5 and layer 2/3 pyramidal neurons were repeatedly imaged every 4 days under ketamine/xylazine anaesthesia (70% of implant surgery dose), starting on average 16 days after surgery. A subset of mice was imaged at 2-day intervals. High-resolution image stacks (1024×1024 pixel, 90×90 μm<sup>2</sup>, 0.5 μm z-step size) of several apical dendrites 10 to 100 μm below the cortical surface (layer 1) were obtained with Fluoview software (Olympus), using a custom-built microscope, a Ti:sapphire laser (Mai Tai, Spectra-Physics) at 910 nm wavelength, focused through a 40 immersion objective (IR, 0.8 NA, Olympus). Lower-magnification image stacks (512×512 pixel, 350×350 μm<sup>2</sup>, 1-2 μm z-step size) of labelled cells were taken and matched to the blood vessel pattern on the brain surface, to relocate imaging regions and to determine the cortical depth of the cell bodies of imaged neurons.

To induce MD, the left lid (contralateral to the imaged hemisphere) was sutured shut immediately after the imaging session. The eye was re-opened 8 days later, immediately following the imaging session. In a subset of mice, a second 8-day MD in the same eye was induced 2-3 weeks later. Imaging was continued between deprivation periods. Another group of animals was imaged 9 times every 4 days before an eye was closed for 8 days to yield control data ("late control", Fig. 4b,d).

### Data analysis

All clear protrusions from the dendrite, irrespective of their orientation relative to the imaging plane, were included in the analysis, resulting in a total of 10548 spines from 100 cells that were tracked over 5-14 imaging sessions. Spine analysis was carried out on raw image stacks in ImageJ, blind with respect to cell position in the cortex. The rate of spine gain and loss is the percentage of spines that appeared and disappeared in between two successive imaging sessions (in a 4-day or 2-day period), relative to the total spine number of the previous imaging session. To investigate if structural changes occurring during MD outlast the 8 day deprivation period (Fig. 3b,c,d, Fig. 4a,c), only those cells were included which were imaged over at least 9 time points and which showed a detectable effect on spine dynamics during MD.

Imaging stacks were aligned with the intrinsic signal response maps via the blood vessel pattern to determine the position of dendritic stretches and cell bodies with regard to cortical region (binocular visual cortex, monocular primary visual cortex, outside primary visual cortex).

To follow the size of spines over time, only spines which clearly protruded from the dendritic shaft on all time points after their appearance were included in the analysis. In the best focal section, intensity values of all pixels comprising the spine were summed after

background subtraction (taken from a region close to the spine which was devoid of GFP-labelled structures). This integrated spine intensity was divided by the mean intensity of the adjacent dendritic shaft to correct for varying imaging conditions. Repeating this analysis with a maximum-intensity projection of all sections containing the spine (instead of the best focal section) yielded very similar results. To compare the size of persistent new spines in MD and control animals to other spines in their vicinity after 8 days of MD (or the equivalent imaging time point for control animals), the integrated spine brightness values of 10 spines on the same dendrite closest to a persistent new spine were included for this analysis (n=130 spines, 13 neurons).

P-values were calculated with a non-parametric Wilcoxon rank sum test for independent samples, with a repeated measures analysis of variance and Wilcoxon sign rank test for paired samples, and with a Dunnett test for comparing different groups to one reference group.

## Supplementary Material

Refer to Web version on PubMed Central for supplementary material.

## Acknowledgements

We thank Tara Keck for contributing control data for Supplementary Figure 5a as well as Max Sperling and Bruno Pichler for programming help. This work was supported by the Max Planck Society, the Wellcome Trust and the Humboldt Foundation.

## References

1. Wiesel TN, Hubel DH. Single cell responses in striate cortex of kittens deprived of vision in one eye. *J. Neurophysiol.* 1963; 26:1003–1017. [PubMed: 14084161]
2. Clark SA, Allard T, Jenkins WM, Merzenich MM. Receptive fields in the body-surface map in adult cortex defined by temporally correlated inputs. *Nature.* 1988; 332:444–445. [PubMed: 3352741]
3. Hofer SB, Mrsic-Flogel TD, Bonhoeffer T, Hübener M. Prior experience enhances plasticity in adult visual cortex. *Nat. Neurosci.* 2006; 9:127–132. [PubMed: 16327785]
4. Bailey CH, Kandel ER. Structural changes accompanying memory storage. *Annu. Rev. Physiol.* 1993; 55:397–426. [PubMed: 8466181]
5. Yuste R, Bonhoeffer T. Morphological changes in dendritic spines associated with long-term synaptic plasticity. *Annu. Rev. Neurosci.* 2001; 24:1071–1089. [PubMed: 11520928]
6. Trachtenberg JT, et al. Long-term in vivo imaging of experience-dependent synaptic plasticity in adult cortex. *Nature.* 2002; 420:788–794. [PubMed: 12490942]
7. Grutzendler J, Kasthuri N, Gan WB. Long-term dendritic spine stability in the adult cortex. *Nature.* 2002; 420:812–816. [PubMed: 12490949]
8. Majewska AK, Newton JR, Sur M. Remodeling of synaptic structure in sensory cortical areas in vivo. *J. Neurosci.* 2006; 26:3021–3029. [PubMed: 16540580]
9. Holtmaat AJ, et al. Transient and persistent dendritic spines in the neocortex in vivo. *Neuron.* 2005; 45:279–291. [PubMed: 15664179]
10. Sawtell NB, et al. NMDA receptor-dependent ocular dominance plasticity in adult visual cortex. *Neuron.* 2003; 38:977–985. [PubMed: 12818182]
11. Gordon JA, Stryker MP. Experience-dependent plasticity of binocular responses in the primary visual cortex of the mouse. *J. Neurosci.* 1996; 16:3274–3286. [PubMed: 8627365]
12. Hensch TK, et al. Local GABA circuit control of experience-dependent plasticity in developing visual cortex. *Science.* 1998; 282:1504–1508. [PubMed: 9822384]

13. Huang ZJ, et al. BDNF regulates the maturation of inhibition and the critical period of plasticity in mouse visual cortex. *Cell*. 1999; 98:739–755. [PubMed: 10499792]
14. Mrsic-Flogel TD, et al. Homeostatic regulation of eye-specific responses in visual cortex during ocular dominance plasticity. *Neuron*. 2007; 54:961–972. [PubMed: 17582335]
15. Tagawa Y, Kanold PO, Majdan M, Shatz CJ. Multiple periods of functional ocular dominance plasticity in mouse visual cortex. *Nat. Neurosci*. 2005; 8:380–388. [PubMed: 15723060]
16. Fischer QS, Graves A, Evans S, Lickey ME, Pham TA. Monocular deprivation in adult mice alters visual acuity and single-unit activity. *Learn. Mem*. 2007; 14:277–286. [PubMed: 17522016]
17. Mataga N, Mizuguchi Y, Hensch TK. Experience-dependent pruning of dendritic spines in visual cortex by tissue plasminogen activator. *Neuron*. 2004; 44:1031–1041. [PubMed: 15603745]
18. Feng G, et al. Imaging neuronal subsets in transgenic mice expressing multiple spectral variants of GFP. *Neuron*. 2000; 28:41–51. [PubMed: 11086982]
19. Wang Q, Burkhalter A. Area map of mouse visual cortex. *J. Comp Neurol*. 2007; 502:339–357. [PubMed: 17366604]
20. Heimel JA, Hartman RJ, Hermans JM, Levelt CN. Screening mouse vision with intrinsic signal optical imaging. *Eur. J. Neurosci*. 2007; 25:795–804. [PubMed: 17328775]
21. Holtmaat A, Wilbrecht L, Knott GW, Welker E, Svoboda K. Experience-dependent and cell-type-specific spine growth in the neocortex. *Nature*. 2006; 441:979–983. [PubMed: 16791195]
22. Knudsen EI. Instructed learning in the auditory localization pathway of the barn owl. *Nature*. 2002; 417:322–328. [PubMed: 12015612]
23. Linkenhoker BA, der Ohe CG, Knudsen EI. Anatomical traces of juvenile learning in the auditory system of adult barn owls. *Nat. Neurosci*. 2005; 8:93–98. [PubMed: 15608636]
24. Knott GW, Holtmaat A, Wilbrecht L, Welker E, Svoboda K. Spine growth precedes synapse formation in the adult neocortex in vivo. *Nat. Neurosci*. 2006; 9:1117–1124. [PubMed: 16892056]
25. Nägerl UV, Kostinger G, Anderson JC, Martin KA, Bonhoeffer T. Protracted synaptogenesis after activity-dependent spinogenesis in hippocampal neurons. *J. Neurosci*. 2007; 27:8149–8156. [PubMed: 17652605]
26. Kasai H, Matsuzaki M, Noguchi J, Yasumatsu N, Nakahara H. Structure-stability-function relationships of dendritic spines. *Trends Neurosci*. 2003; 26:360–368. [PubMed: 12850432]
27. Bourne J, Harris KM. Do thin spines learn to be mushroom spines that remember? *Curr. Opin. Neurobiol*. 2007; 17:381–386. [PubMed: 17498943]
28. Matsuzaki M, Honkura N, Ellis-Davies GC, Kasai H. Structural basis of long-term potentiation in single dendritic spines. *Nature*. 2004; 429:761–766. [PubMed: 15190253]
29. Kopec CD, Li B, Wei W, Boehm J, Malinow R. Glutamate receptor exocytosis and spine enlargement during chemically induced long-term potentiation. *J. Neurosci*. 2006; 26:2000–2009. [PubMed: 16481433]
30. Zhou Q, Homma KJ, Poo MM. Shrinkage of dendritic spines associated with long-term depression of hippocampal synapses. *Neuron*. 2004; 44:749–757. [PubMed: 15572107]



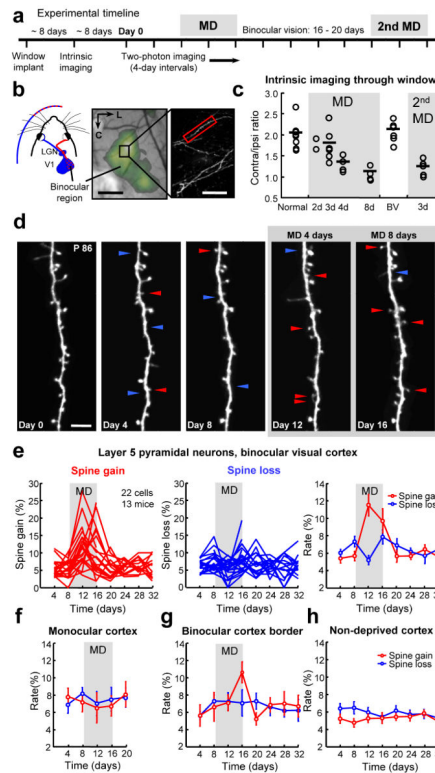


**Figure 1. Monocular deprivation in adult mice increases the rate of spine addition in layer 5 neurons in binocular cortex**

**a**, Timeline of the experimental protocol. **b**, Schematic of the mouse visual system (left), intrinsic signal map of the binocular visual cortex (middle, scale bar: 500  $\mu\text{m}$ ) and low-magnification image of a L5 neuron apical dendrite (right, scale bar: 50  $\mu\text{m}$ ). **c**, OD shifts during contralateral eye MD, 1-2 weeks after eye re-opening (BV: binocular vision) and during a second MD, measured by intrinsic signal imaging and shown as ratio of contralateral to ipsilateral eye response strength (contra/ipsi ratio). Circles depict data from individual mice, horizontal lines indicate mean values. **d**, High-magnification view of the dendritic stretch shown in **b** (red box), imaged every 4 days (depth  $\sim 25 \mu\text{m}$ , soma depth  $\sim 625 \mu\text{m}$ ). MD in the contralateral eye was induced at the end of the third imaging session (day 8). Arrows point to spines appearing (red) or disappearing (blue) compared to the previous imaging session. Scale bar: 5  $\mu\text{m}$ . **e-h**, Percentage of spines appearing (spine gain) and disappearing (spine loss) on layer 5 neurons between two imaging time points plotted against time for different cortical regions or conditions: binocular visual cortex (**e**, left, middle: individual neurons; right: average data, 22 cells, 13 mice, 2360 spines), monocular region of primary visual cortex (**f**, 7 cells, 6 mice, 754 spines), border of the binocular region (**g**, 9 cells, 9 mice, 984 spines), and control data from non-deprived mice (**h**, 21 cells, 11 mice, 2468 spines). Error bars denote SEM.

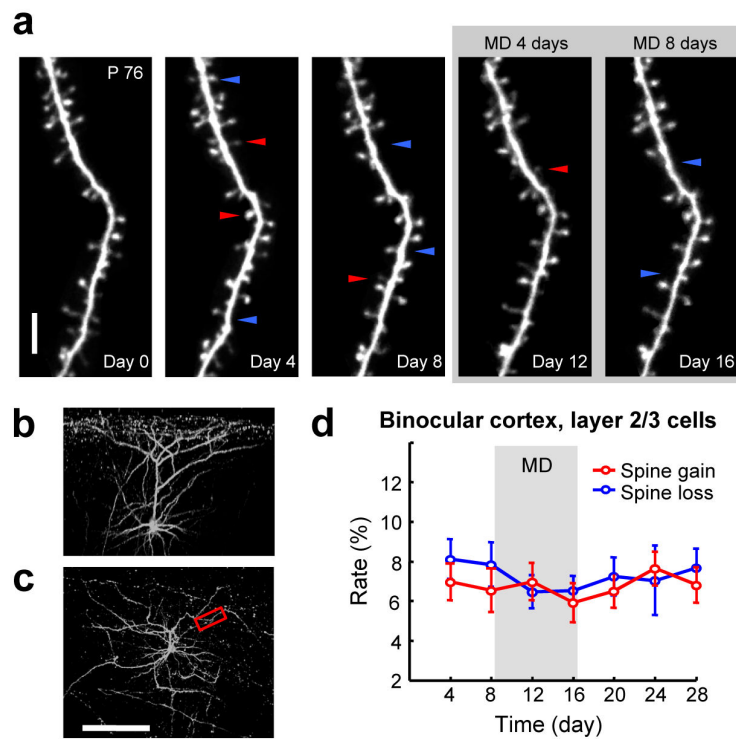


**Figure 2. Monocular deprivation in adult mice does not alter spine dynamics in layer 2/3 neurons**  
**a**, Repeatedly imaged dendritic stretch of a layer 2/3 pyramidal neuron (imaging depth  $\sim 50$   $\mu\text{m}$ , soma depth  $\sim 210$   $\mu\text{m}$ ) shown in **b** (side view) and **c** (top view, red box outlines dendritic stretch shown in **a**, scale bar: 100  $\mu\text{m}$ ). Arrows mark spine changes from previous imaging time point (red: spine gained, blue: spine lost). Scale bar: 5  $\mu\text{m}$ . **d**, Average spine gain and loss on layer 2/3 pyramidal neurons in binocular visual cortex (7 cells, 4 mice, 1101 spines). Error bars denote SEM.

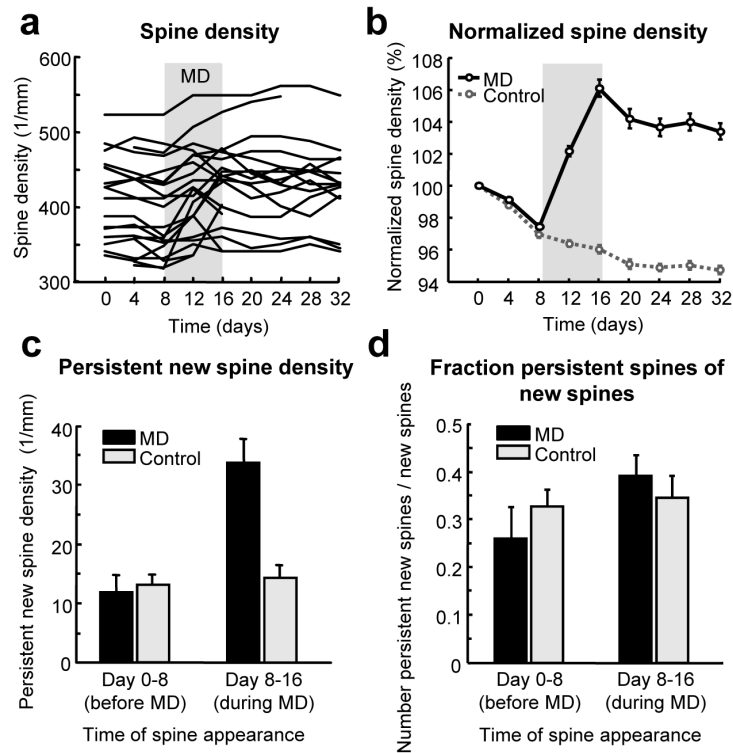


**Figure 3. MD-induced increase in spine density on layer 5 neurons outlasts the altered experience**  
**a**, Spine density as a function of time for all imaged layer 5 neurons in binocular visual cortex (22 cells, 13 mice, 2360 spines). **b**, Average normalized spine density of layer 5 cells showing an increase in spine density during MD, imaged for at least 32 days (black, 14 cells, 9 mice, 1316 spines). **c**, Density of newly appeared spines that remain stable for a minimum of 16 days. The data have been split according to the time when the spines first appeared: before MD, during MD, and during equivalent periods in control animals. **d**, Ratio of persistent new spines to all new spines before and during MD. Matched control data from non-deprived mice are shown in gray. Error bars indicate SEM.

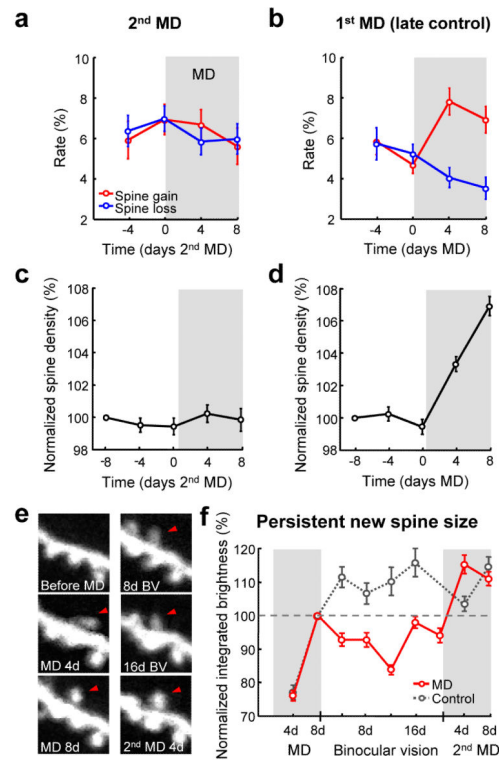


**Figure 4. A second MD increases the size of spines gained during the first MD without additional spine gain**

Rate of spine gain and loss (**a,b**) and normalized spine density (**c,d**) on layer 5 pyramidal neurons during a second period of contralateral-eye MD induced 2-3 weeks after the first (**a,c**, 14 cells, 9 mice, 1316 spines), and during a single MD in control mice of similar implant duration and number of imaging sessions before the MD (**b,d**, 14 cells, 11 mice, 1693 spines). **e**, Example of a spine that appeared during the first 4 days of MD and its brightness/size changes over time. BV: binocular vision. **f**, Average integrated brightness of persistent new spines that appeared during MD (red) or during the corresponding time period in non-deprived control animals (gray), normalized to the spine brightness value at the end of the first MD or the equivalent time point in control mice. Error bars indicate SEM.